J3.1 TURBULENT TRANSPORT OF ^{222}Rn AND ITS SHORT-LIVED DAUGHTERS IN CONVECTIVE BOUNDARY LAYERS

Jean-François Vinuesa*, Stefano Galmarini
Institute for Environment and Sustainability, Joint Research Center, 21020 Ispra, Italy.

1. INTRODUCTION

^{222}Rn is a natural radioactive compound with a half-life of 3.8 days. Its noble gas nature makes it a suitable tracer in studies of atmospheric boundary layers (Porstendörfer, 1994). Ground-based measurements and vertical distributions of ^{222}Rn and its daugthers have been extensively studied in the past, e.g., to characterize the turbulent properties of the ABL, to perform regional and global circulation model benchmarking and to estimate regional surface fluxes of air pollutant and in particular climatically sensitive compounds. For a review on the use of ^{222}Rn observations in atmospheric science see Zahorowski *et al.* (2004). Several studies (e.g., Larson *et al.*, 1972; Lopez *et al.*, 1974; Polian *et al.*; 1986; Gaudry *et al.*, 1990; Ramonet *et al.*, 1996; Galmarini, 2005) have shown that the study of the behavior of radon and its progenety is of great importance for air pollutant and greenhouse gases transport modeling. In particular, ^{222}Rn is often used to calibrate and validate transport model (e.g., Jacob *et al.*, 1997; Dentener *et al.*, 1999).

Some of the radon radio nuclides and their short-lived daughters have been used to study the turbulent diffusion process since they have half-lifes of the same order of magnitude of the turnover time of the convective boundary layer. Compounds with a lifetime comparable to or shorter than that of the turbulent transport, can be inefficiently mixed by the turbulent transport. This process influences the distribution of ^{222}Rn daughters, and in particular their fluxes. Whereas the so-called long lived species are well mixed and the vertical flux profiles follow a linear shape, the short-lived compound fluxes deviate from the inert linear profile. In this respect, accurate modeling requires improved understanding on how turbulence affect the dispersion of ^{222}Rn and its progeny in atmospheric boundary layers. The scales associated with turbulent motions range from the Kolmogorov dissipation scale (on the order of a millimeter) to the boundary layer depth (on the order of a kilometer). The largest eddies are responsible for the turbulent transport of the scalars and momentum whereas the smallest ones are mainly dissipative. Thus, realistic numerical experiments of the atmospheric boundary layer require the use of large-eddy simulation (LES) that allow to explicitly resolve relevant turbulent scales.

To our knowledge, no study so far has analysed the turbulent transport of ^{222}Rn short-lived daughters in a CBL in a comprehensive and complete manner. This paper aims at providing such an analysis. We perform a complete analysis of the vertical distribution, reactivity and turbulent transport of ^{222}Rn and its progeny under convective conditions. In order to account for all the relevant scales of the atmospheric boundary layer, we use LES to explicitely calculate the different terms of the concentration budget equations. In addition, this study is perform on both steady and unsteady conditions represented by a fully developed CBL and a CBL growing within an overlayered reservoir layer resulting of the collapse of previous daytime CBL. The study under steady state conditions allows to perform a ful budget analysis of the turbulent transport and so to identify the driving process of ^{222}Rn and its progeny concentration behavior. The analysis of the unsteady boundary layer aims at understanding the exchanges between the reservoir and the mixed layer while the boundary layer is deepening and so the turbulent timescale is increasing.

2. NUMERICAL SET-UP

2.1 ^{222}*Rn decaying chain*

We consider the radioactive decay chain of ^{222}Rn that reads

$$^{222}Rn \xrightarrow{\lambda_0} {}^{218}Po \xrightarrow{\lambda_1} {}^{214}Pb \xrightarrow{\lambda_2} {}^{214}Bi \xrightarrow{\lambda_3} {}^{210}Pb, \quad (1)$$

where λ_0, λ_1, λ_2 and λ_3 are the decay frequency equal to 2.11 x 10^{-6}, 3.80 x 10^{-3}, 4.31 x 10^{-4}, and 5.08 x 10^{-4} s^{-1}, respectively. Note that we consider a direct transformation of ^{214}Bi into ^{210}Pb since the half-life of ^{214}Po (daughter of ^{214}Bi) is very short (164 μs). Also we consider ^{210}Pb, that have a half-life of 22.3 years, as an inert scalar with respect to the temporal scales considered here. To increase readability, ^{222}Rn and its progeny will be also referred to as S_i where i is the rank of the daughter in the decay chain from here on, e.g. S_0 and S_4 stand for ^{222}Rn and ^{210}Pb, respectively.

In the atmosphere, under horizontally homogeneous conditions with no mean wind and neglecting that transport due to molecular diffusion, the temporal evolution of a compound S_i involved in the previously presented radioactive system reads

$$\frac{\partial S_i}{\partial t} = -\frac{\partial \overline{ws_i}}{\partial z} + R_{S_i} \quad (2)$$

where the horizontal averages are denoted by capital letters and the fluctuations of the variables around the horizontal average value by lower case letters. The radioactive source/sink terms R_{S_i} are

* *Corresponding author address:* Jean-François Vinuesa, IES - HO4 - REM - TP441, Joint Research Center, Via E. Fermi 1, 21020 Ispra (VA), Italy.; e-mail: jeff.vinuesa@jrc.it.

$$R_{S_0} = -\lambda_0 \, S_0, \tag{3}$$
$$R_{S_1} = \lambda_0 \, S_0 - \lambda_1 \, S_1, \tag{4}$$
$$R_{S_2} = \lambda_1 \, S_1 - \lambda_2 \, S_2, \tag{5}$$
$$R_{S_3} = \lambda_2 \, S_2 - \lambda_3 \, S_3, \tag{6}$$
$$R_{S_4} = \lambda_3 \, S_3. \tag{7}$$

2.2 *Numerical simulations*

Two representative cases are investigated: a fully developed free convective atmospheric boundary layer and a CBL growing overlayed by a reservoir layer resulting from the collapse of the previous daytime CBL. For both cases, the modeling domains represent $6.4\ km$ x $6.4\ km$ x $1.5\ km$ with a vertical and horizontal resolutions of 25 and 50 meters respectively, leading to 128 x 128 x 60 gridpoints simulations. Periodic lateral boundary conditions are assumed. The maximum time-step used in the calculations is $0.5\ s$.

The simulated ABLs are dry (as radon and its daughters are unaffected by moisture) convective ABLs driven by buoyancy only (see Table 1).

	Steady-state CBL	Unsteady CBL
	(1)	(2)
z_i	$662.5\ metres$	$187.5\ metres$
Θ_m	$288\ K$	$286\ K$
$\Delta\Theta$	$5\ K$	
$(\overline{w\theta})_s$	$0.052\ K\ m\ s^{-1}$	
γ_θ	$6\ 10^{-3}\ K\ m^{-1}$	

Table 1: Initial values and prescribed surface fluxes used for both simulations.

In the steady-state CBL, ^{222}Rn is emitted at the surface with a flux of $0.5\ Bqm^{-2}s^{-1}$. All radioactive compounds have a zero initial profile except ^{222}Rn. This latter profile is the result of a pre-run of 1 hour simulation with the same surface flux, no initial concentration and a decay constant set to zero. The simulation is running for 8 hours with a presimulation of 1 hour for the dynamics. The statistics are done on the last hour of the simulation. The convective velocity scale w_*, the ABL height z_i and the free convection time-scale $t_* \equiv z_i/w_*$ are equal to $1.12\ ms^{-1}$, $800\ m$ and $714.3\ s$, respectively.

For the unsteady convective BL, we follow a special procedure to initialize ^{222}Rn and its daughters profiles in order to ensure consistency regarding the assumption of radioactive equilibrium of ^{222}Rn and its progeny. ^{222}Rn and its daughters profile concentrations are analytically calculated as the result of a 8 hours of radioactive activity from the resulting profiles of the previously simulated steady-state CBL . Since the reservoir layer is assumed decoupled from the surface, no fresh radon is transported to this region during the night. However in the CBL, the ^{222}Rn surface flux of $0.5\ Bqm^{-2}s^{-1}$ in the nocturnal boundary layer is assumed constant during the 8-hours night. The simulation is running for 8 hours.

2.3 *Reacting turbulent flow classification*

Previous studies (e.g. Schumann, 1989; Vilà-Guerau de Arellano, 2003) have shown that turbulent reacting flows can be classified using the so-called turbulent Damköhler number Da_t, defined as the ratio between the integral time-scale of turbulent (τ_t) and the chemical time-scale (τ_c). For reacting flows with $Da_t << 1$, the chemical transformations proceed at a slower rate than the turbulent mixing. Therefore, there is little influence of the turbulent structures on the chemistry and the reacting flow is in a so-called slow chemical regime. When $Da_t \approx O(1)$, i.e. the time-scale of the chemistry is of similar order to the time-scale of the turbulent mixing, atmospheric turbulence controls chemical reactivity. As a consequence, the behavior of chemically active species can differ from the behavior observed and modelled of inert scalars. For $Da_t >> 1$, chemical transformations are much faster then the turbulent mixing of the reactants that chemical species react in-situ and are almost not transported. In our simulations, $\tau_t = z_i/w_*$ and $\tau_c = \lambda_j^{-1}$ with j=0, 1, 2, and 3. The corresponding Da_t are summarized in Table 2. These numbers indicate that ^{218}Po (S_1) is strongly influences by the turbulent structure of the ABL in both steady and unsteady conditions. The other short-lived daughters, i.e. ^{214}Pb (S_2) and ^{214}Bi (S_3), Da_t refer to a moderate-slow regime indicating that their distribution is only slightly affected by the control exert by turbulent on their radioactive decay.

Compounds	Steady-state CBL	Unsteady CBL
S_0	< 0.01	< 0.01
S_1	2.71	1.21-2.24
S_2	0.31	0.14-0.25
S_3	0.36	0.16-0.30

Table 2: Volume averages of the turbulent Damköhler numbers.

While studying the relevance of accounting for the chemical contribution to second-order moments (fluxes and (co-)variances) of reacting scalars, Vinuesa and Vilà-Guerau de Arellano (2003) derived dimensionless numbers, the so-called Damköhler numbers for fluxes and (co-)variances. These numbers are based on the chemical terms for second-order moment budget equations. They showed that for flux and (co-)variance Damköhler numbers $\sim O(1)$, the contribution of chemical terms to second-order moment profiles is significant. The flux Damköhler number can be expressed as the ratio of the flow time-scale to the time-scale of the chemical contribution to the flux. For instance for a scalar B involved the chain

$$A \overset{\lambda_A}{\rightarrow} B \overset{\lambda_B}{\rightarrow} C, \tag{8}$$

the flux Damköhler number for the scalar B reads

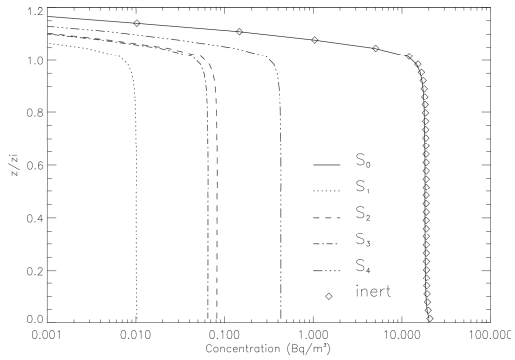

FIG. 1: Vertical profiles of ^{222}Rn (S_0) and its progeny. The solid line accounts for the concentration of an inert scalar that as the same surface flux as S_0.

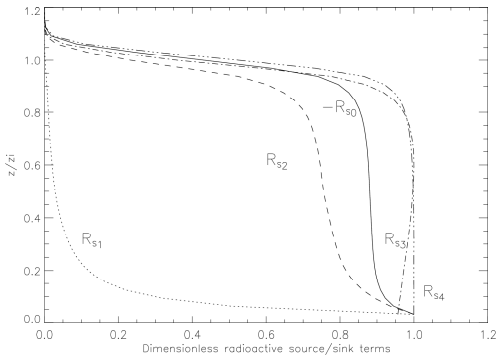

FIG. 2: Vertical profiles of the radioactive decay contribution to the concentration budget equations. The profiles are made dimensionless by using their maximum value. Note that the minus decay term of the S_0 concentration budget is plotted to increase readability.

$$Da_{\overline{wb}} = \left| Da_{t,B} - Da_{t,A} \frac{w_* s_{a*}}{w_* s_{b*}} \right| . \qquad (9)$$

By calculating the $w_* s_{i*}$ as proposed by Cuijpers and Holtslag (1998), i.e. $w_* s_{i*} = \frac{1}{z_i} \int_0^{z_i} \overline{ws_i} dz$, we calculate the flux Damköhler numbers and report them in Table 3. In the steady state CBL, significant effects of the radioactive decay contribution on the flux for ^{218}Po (S_1) and ^{214}Pb (S_2) can be expected whereas ^{214}Bi (S_3) flux Damköhler number only indicates a small contribution in the steady state CBL. However, under unsteady conditions only S_1 flux should show some impact of the radioactive decay contribution.

Compounds	Steady-state CBL	Unsteady CBL
S_0	< 0.01	< 0.01
S_1	1.08	0.62-0.38
S_2	0.85	0.06-0.09
S_3	0.16	0.01-0.02
S_4	< 0.01	< 0.01

Table 3: Volume averages of the flux turbulent Damköhler numbers.

3. DISPERSION OF ^{222}Rn AND ITS PROGENY IN THE STEADY-STATE CBL

As one can notice in Figure 1 where the vertical profile of ^{222}Rn (S_0) and its progeny are shown, the mixed-layer concentrations are correlated with the half-lifes of the compounds; the faster decaying the daughter is, the smaller is the concentration. Also as indicated by the Damköhler number classification, S_0 concentration only shows a small deviation from the inert scalar one. All the compounds show well-mixed profiles however and since a wide range of radioactive decay constant is considered, e.g. from some minutes to days, any and even very smal discrepancy in height can have important impacts on the reactivity.

We explicitely calculate the radioactive decay contribution to the concentrations and we show the resulting profiles in Figure 2. As can be expected for S_0 and since its radioactive decay contribution is proportional to its concentration, the radioactive decay is acting as a sink with a constant value whithin the mixed layer. For radon's daughters, the radioactive decay terms are a balance between product by the decay of their father and destruction but their own radioactive decay. For all the daughters, the radioactive decay contribution show an unbalance in favor of their production. Thus, as long as S_0 is injected in the steady-state CBL, their concentration will grow with time. However, one can notice that the daughters' vertical profiles are quite different and that, apart S_4, none of them show a well-mixed behavior.

Since S_1 is the first daughter of the serie, its production by the decay of S_0 is more important where the ^{222}Rn concentrations are higher, i.e. close to the surface. The radioactive decay of S_1 proceeds at a faster rate than the turbulent mixing meaning that freshly created S_1 are decaying before being well mixed in the CBL. As a result, the shape of the profile is quite different for the S_0 one showing a fast reduction while moving upward. For the daughters with a longer half-life than S_1, turbulence is more efficient to mix freshly created compounds with older ones but still some discrepancy in height can be noted for S_2 and S_3.

Actually, for this latter, one can notice a very interesting behavior: while all other radioactive contributions are more important close to the surface, the one of S_3 shows a maximum contribution at $0.6 - 0.7\ z/z_i$. Since S_4 radioactive decay contribution show a constant profile at lower altitudes and since it is proportional to S_3 concentration, one can assume that S_3 is well-mixed in the CBL. As mentioned previously, the decaying term in the S_3 concentration budget equation is composed of a source term and a sink term. The source term is the production by radioactive decay of S_2 and the sink term is

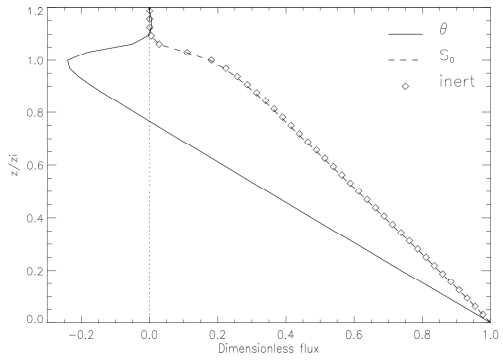

FIG. 3: Vertical profiles of the dimensionless fluxes. S_0 and an inert scalar s fluxes are plotted using dashed and diamond lines, respectively. Both compounds are emitted with the same surface fluxes. The sensible heat flux is also shown and is represented by a solid line. The values are made dimensionless by $w_*\theta_*$ for the temperature and $w_* s_{i*}$ for the chemical fluxes where w_*, θ_* and s_{i*} are the convection velocity scale, the temperature scale and the concentration scale defined as the ratio of the surface flux of S_0 to the convection velocity scale.

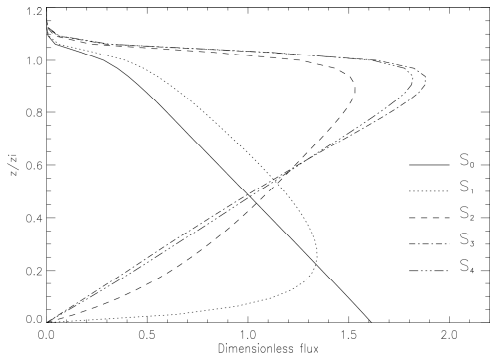

FIG. 4: Vertical profiles of the dimensionless fluxes for ^{222}Rn (S_0) and its daughters. The values are made dimensionless by $w_* s_{i*}$ as proposed by Cuijpers and Holtslag (1998).

its own radioactive decay that is equal to the radioactive decay production of S_4. Thus the maximum total S_3 radioactive contribution in the upper boundary layer is due to the enhanced production by radioactive decay of S_2 and we can conclude that S_2 is also inefficiently mixed by turbulence.

Figure 3 shows the vertical profiles of the inert scalar, ^{222}Rn (i.e., S_0) and temperature fluxes. Within the boundary layer, the profiles of inert scalars have a linear shape (Deardorff, 1979; Wyngaard and Brost, 1984) whereas the fluxes of reacting scalars show deviations with from this shape correlated with their Damkhöler numbers (Gao and Wesely, 1994; Sykes et al., 1994; Vinuesa and Vilà-Guerau de Arellano, 2003). These deviations are due to the action of the chemistry that can act as a sink or a source term in the flux budget. The flux of ^{222}Rn is similar to the inert scalar flux. Thus the chemical term, that is the radioactive decay in our case, has no impact on the vertical transport of ^{222}Rn as its Damköler and flux Damköler numbers suggested with $Da_t < 0.01$ and $Da_{\overline{ws_0}} < 0.01$.

The fluxes of S_0 and its progeny are shown in Figure 4. The fluxes of S_0 and S_4 have a linear profile whereas the other daughter fluxes show deviations from the linear shape. As mentioned previously, the deviations of radon's progeny fluxes from the inert linear shape are correlated with the Damköhler numbers. S_1 has the highest Damköhler number ($Da_t = 2.71$) and its flux shows the biggest deviation. The other short-lived daughters, i.e. S_2 and S_3, have similar Da_t but while the deviation of S_2 flux is significant, the ones of S_3 is rather small. Using the appropriate Damköhler number to assess the relevance of radioactive decay contribution to the flux allows to clarify this discrepancy. The flux Damköhler number for S_2 read 0.85 while the one of S_3 equals 0.16 suggesting the vertical transport of S_2 is the one most significantly affected by turbulence.

The most interesting point is that the vertical distribution of the fluxes change from one daughter to another. For radon, the maximum flux is found at the surface where radon is emitted. Since all daughters are produced by the radioactive decomposition of S_0, one should expect to find maximum daughter fluxes close to the surface. However, this is not the case and the maximum flux location is moving upwards while the rank of the daughter in the ^{222}Rn progity is increasing. ^{218}Po has its maximum flux at $0.25\ z/z_i$ and the others daughters maximum fluxes are located around $0.9\ z/z_i$. Actually, the maximum flux location reaches a quasi steady state value betwen 0.90 and $0.95\ z/z_i$ for the slowest (in the flux Damköhler number sense) daughters, i.e., S_3 and S_4.

4. DISPERSION OF ^{222}Rn AND ITS PROGENY UNDER UNSTEADY CONDITIONS

In Figure 5, we show the time evolution of the concentration of the father ^{222}Rn (S_0) and the last daughter of the chain ^{210}Pb (S_4). The other daughters are not shown since they have the same overall behavior as S_0. No fresh emissions of S_0 reach the reservoir layer since it is almost decoupled from the surface. As a result, S_0 (and its daughters except S_4) concentration decreases with time. Since S_4 is the last daughter of the chain and is considered as an inert scalar, its concentration increases with time following the chain decaying process.

As the boundary layer deepens with time, the S_0 concentration collapses despite of fresh emission. This collapse is due to both the dilution of S_0 in an increasing volume and the entrainment of S_0 low concentration air from the reservoir layer. The same behavior is observed for the other daughters except S_4. The concentration of this latter is the result of antagonist effects: the production by the decaying chain, the dilution by boundary layer deepening and the entrainment of lower concentration air masses from the reservoir layer. Its concentration in the

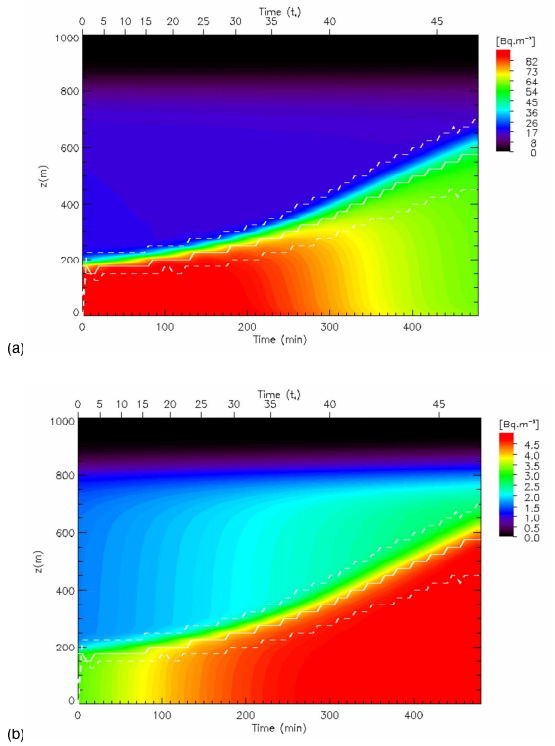

FIG. 5: Vertical profiles of (a) ^{222}Rn (S_0) and (b) ^{210}Pb (S_4) concentrations. The top of the CBL is overplotted with a white solid line and the entrainment layer is located between the dashed white lines. The step aspect of these latter quantities is due to averaging procedures, e.g. the CBL depth and the entrainment layer location are determined from the 5 minutes slab averaged sensible heat flux. The concentrations are plotted against time in minutes (lower x-axis) and in t_* (upper x-axis) where $t_* = z_i/w_*$.

reservoir layer increases with time and, as it can be noticed in Figure 5b, it is comparable with its concentration in the boundary layer. However, the reservoir layer concentration remains lower then the boundary layer one meaning that the entrainment of upper air masses still dilutes the CBL concentration. Thus, the combined effect of dilution and entrainment do not balance the production by the radioactive decay and, as a result, S_4 concentration increases with time in the CBL.

5. CONCLUSION

The effect of turbulent transport in convective boundary layers on the distribution of ^{222}Rn and its progeny has been studied performing large-eddy simulation of steady-state and unsteady boundary layers. The analysis of the concentration budget reveals that the concentrations are correlated with the half-life of the radioactive compounds and that the short-lived daughters vertical distribution and vertical flux can be affected by the turbulent structure of the atmospheric boundary layer.

Under steady state conditions, we found a discrepancy with height while focusing on the radioactive decay contributions to the concentrations. The exact decomposition of the flux budget under steady-state revealed that while ^{222}Rn show the typical bottom-up scalar flux behavior, ^{210}Pb exhibits the one of a top-down scalar. We also found that ^{222}Rn short-lived daughters, e.g. ^{218}Po and ^{214}Pb, have relevant radioactive decaying contributions acting as flux sources leading to deviations from the linear flux shape.

Under unsteady conditions, ^{222}Rn and its progeny concentrations collapse due to the growth of the boundary layer. While we found comparable behaviors as in the steady state CBL for the radioactive decay contributions to the concentrations, the fluxes are affected by the deepening of the CBL. Our analysis revealed the crucial role of turbulent transport and, in particular entrainment, on the morning concentrations of ^{222}Rn and its daugthers.

REFERENCES

Cuijpers, J. W. M. and A. A. M. Holtslag, 1998: Impact of skewness and nonlocal effects on scalar and buoyancy fluxes in convective boundary layers, *J. Atmos. Sci.,* **55**, 151-162.

Deardorff, J. W., 1979: Prediction of convective mixed-layer entrainment for realistic capping inversion structure, *J. Atmos. Sci.,* **36**, 424-436.

Dentener, F., Feichter, J. and A. Jeuken, 1999: Simulation of the transport of Rn-222 using on-line and off-line global models at different horizontal resolutions: a detailed comparison with measurements, *Tellus,* **51B**, 573-602.

Galmarini, S., 2005: One Year of 222-Rn Concentration in the Atmospheric Surface Layer, *Atmos. Chem. Phys. Discuss.*, **5**, 12895-12937.

Gao, W. and M. L. Wesely, 1994: Numerical modelling of the turbulent fluxes of chemically reactive trace gases in the atmospheric boundary layer, *J. Appl. Meteorol.,* **33**, 835-847.

Gaudry, A., G. Polian, B. Ardouin and G. Lambert, 1990: radon-calibrated emissions of CO2 from South Africa. *Tellus,* **42B**, 9-19.

Jacob, D.J., M.J. Prather, P.J. Rasch, R.L. Shia, Y.J. Balkanski, S.R. Beagley, D.J. Bergmann, W.T. Blackshear, M. Brown, M. Chiba, M.P. Chipperfield, J. deGrandpre, J.E. Dignon, J. Feichter, C. Genthon, W.L. Grose, P.S. Kasibhatla, I. Kohler, M.A. Kritz, K. Law, J.E. Penner, M. Ramonet, C.E. Reeves, D.A. Rotman, D.Z. Stockwell, P.F.J. VanVelthoven, G. Verver, O. Wild, H. Yang and P. Zimmermann, 1997: Evaluation and intercomparison of global atmospheric transport models using Rn-222 and other short-lived tracers, *J. Geophys. Res.*, **102**, 5953-5970.

Larson, R. E., R. A. Lamontagne and W. I. Wittmann, 1972: Radon-222, CO, CH4 and continental dust over the greenland and norwegian seas, *Nature,* **240**, 345347.

Lopez, A., D. Guedalia, J. Servant and J. Fontan, 1974: Advantages of the use of radioactive tracers 222Rn and 212Pb for the study of aitken nuclei within the lower troposphere, *J. Geophys. Res.,* **79**, 12431252.

Polian, G., G. Lambert, B. Ardouin and A. Jegou, 1986:

Long-range transport of continental radon in subantarctic and antarctic areas, *Tellus,* **38B**, 178-189.
Porstendörfer, J., 1994: Properties and behaviour of radon and thoron and their decay products in the air, *J. Aero. Sci.,* **25**, 219-263.
Ramonet, M., J. C. Le Roulley, P. Bousquet and P. Monfray, 1996: Radon-222 measurements during the Tropoz II campaign and comparison with a global atmospheric transport model, *J. Atm. Chem.,* **23**, 107136.
Schumann, U., 1989: Large-eddy simulation of turbulent diffusion with chemical reactions in the convective boundary layer, *Atmos. Environ.,* **23**, 1713-1729.
Sykes, R. I., S. F. Parker, D. S. Henn and W. S. Lewellen, 1994: Turbulent mixing with chemical reactions in the planetary boundary layer, *J. Appl. Meteorol.,* **33**, 825-834.
Vilà-Guerau de Arellano, J., 2003: Bridging the gap between atmospheric physics and chemistry in studies of small-scale turbulence, *Bull. Amer. Meteor. Soc,* **84**, 51-56.
Vinuesa, J.-F. and J. Vilà -Guerau de Arellano, 2003: Fluxes and (co-)variances of reacting scalars in the convective boundary layer, *Tellus,* **55B**, 935949.
Wyngaard, J. C. and R. A. Brost, 1984: Top-down and bottom-up diffusion of a scalar in the convective boundary layer, *J. Atmos. Sci.*, **41**, 102–112.
Zahorowski, W., S.D. Chambers and A. Henderson-Sellers, 2004: Ground based radon-222 observations and their application to atmospheric studies, *J. Env. Rad.,* **76**, 3-33.